Investigating the effect of salt concentrations on the immune cell membrane protein CD45 D1-D4 in a supported lipid bilayer using hydrodynamic trapping

LUND UNIVERSITY
Faculty of Science

Bachelor of science thesis (15 hp) 2017

Author: Carl-Eric Onema

Supervisors: Dr. Peter Jönsson and Victoria Junghans

Examiner: Prof. Malin Zackrisson Oskolkova

Department of Physical Chemistry

Lund University

Abstract

The immune system is a very complex system, aimed to protect the body from the many dangers that loom around us. A well-functioning immune system can fight of most invaders, remove foreign particles that entered our bodies, and take care of dead cells.

The aim in this work is seeing how the protein CD45 (also known as PTPRC, protein tyrosine phosphatase, receptor type, C) is affected by salt concentration, more exactly how it is oriented on a lipid bilayer. CD45 have been observed to be essential for proper activation of T cells, but exactly how this is achieved on a molecular level is not known. Since the protein interact with its environment, its orientation may play an important role for the sensitivity and function of CD45.

In order to investigate this, a combination of total internal reflection fluorescence microscopy, FRAP (fluorescence recovery after photobleaching) and hydrodynamic trapping have been used. The protein was attached to a supported lipid bilayer (SLB), which is a common cell membrane mimic. The orientation of the protein, i.e. its effective height, on the bilayer was measured using hydrodynamic trapping at different concentrations of sodium chloride at a physiological pH of 7.4. The diffusion of the protein across the SLB was also studied at different salt concentrations. The investigation implied a difference in the height of the proteins with it standing higher above the bilayer with increased salt concentration. This finding is important since it has consequences for how CD45 should be modelled on cell membrane mimics such as SLBs as well as on live cells.

Abbreviations

SLB	Supported lipid bilayer
TIRFM	Total internal reflection fluorescence microscope
FRAP	Fluorescence recovery after photobleaching
CD45	Cluster of differentiation 45. CD45 D1-D4 will be called CD45 in the text
PTPRC	Protein tyrosine phosphates, receptor type, C
DGS-NTA	1,2-dioleoyl-*sn*-glycero-3-[(N-(5-amino-1-carboxypentyl)iminodiacetic acid)succinyl] (nickel salt)
POPC	1-palmitoyl-2-oleoyl-sn-glycero-3-phosphocholine
HEPES	4-(2-hydroxyethyl)-1-piperazineethanesulfonic acid)

Populärvetenskaplig sammanfattning

Många av dem mest spektakulära händelserna som sker i vår värld kan inte ses med blotta ögat. Vid varje andetag sker miljontals reaktioner, saltkoncentrationen i cellerna regleras, signaler skickas genom kroppens nervsystem, och receptorer plockar upp signalmolekyler likt hur post skickas till brevlådan och läses av oss i hemmet.

Immunförsvaret är en otroligt viktig del av vår kropp som dagligen handskas med olika inkräktare som tar sig in i kroppen. Det ser till att sålla bort det som inte ska vara i kroppen likt hur reklamen sållas bort när det står ”ingen reklam” fastklistrat på brevlådan, eller så som spamfiltret i din e-post gör att mail med skadliga länkar hamnar i skräpposten.

Tänk dig nu att du ska hantera posten som kommer till hela ditt kvarter, eller låt säga att du ska hantera brevflödet som skickas till 100 personer, och det gäller att du sållar bort den oönskade reklamen. Du kan göra det själv, eller ta hjälp utav andra men när du gör detta måste du förse dem du tar hjälp av med energi och se till att de går hem igen när de inte finns något att göra så de inte blir rastlösa och börjar löpa amok! Lite så fungerar det med immunförsvaret. Det måste kunna svara i rätt proportioner, annars väntar problem.

I detta arbetet undersöktes en aspekt i immunförsvarets led som hanterar regleringen och initialiseringen av T-celler, B-celler samt andra typer av blodceller och går under namnet CD45. Protein har olika områden, aktiva säten, där reaktioner sker. Intresset för arbetet låg i att se hur en del av proteinet, CD45 D1-D4, orienterade sig i olika saltkoncentrationer med hjälp av en metod kallad ”*Hydrodynamic Trapping*”, en generell proteinfälla som utan direkt kontakt med proteinet samlar upp dem vid en punkt på en konstgjord cellyta kallad ”*supported lipid bilayer”*.

CD45 är ett protein som enbart finns på blodceller och på immunceller återfinns proteinet i ofantliga mängder. CD45 har i uppgift att slå på och av immuncellernas aktivitet då vissa immunceller kan vara för starka även för vår egen kropp. Att veta hur detta protein fungerar är av stor betydelse då immunförsvaret har stor betydelse för att vi ska kunna leva ett friskt liv.

Contents

1 Introduction

Many of the most amazing things in this world cannot be seen by our eyes. For every breath we take, millions upon millions of reactions take place, ions are shuffled in and out of cells, signals are sent through our nerves and receptors in our cells take up signal molecules. Knowing how these systems work on a molecular level is of great importance as it can be the difference between life and death.

It is well known that cells can communicate with one other either by picking up signals through nerves or by signalling molecules that travel through the blood or the lymphatic system and is detected by a receptor.

Every person consists of a vast number of complex systems that are regulated by various mechanisms, and the study of these processes in our body is of great importance for our understanding of how we function. Studying protein interactions is no easy task and it requires much work to be done before finally being able to do research on them. A diagnosis must be set by a physician, the culprit, usually a protein, has to be isolated and the gene needs to be identified.

Many diseases in our world is due to genetic defects in the DNA which in turn may lead to improperly folded proteins. As a result, the function of the protein can become less efficient, it can be lost, or it can even become self-damaging. Proteins come in various forms and perform many different tasks. Some function as channels which helps regulate the flow of ions across the cell membranes either by passive transport or by active transport through potential gradients. Other protein works as enzymes, catalysing the slowest of reactions to occur at incredible speed and there is a class of proteins that work for signalling purposes, allowing for fast communication of different regulatory systems within the body.

The aim of this project is to see how the height of the CD45 D1-D4 (referred to as CD45 for the remainder of the text) protein is affected by varying the concentration of salt in the buffer solution set at a physiological pH of 7.4. The molecular structure of this molecule is shown in Figure 1. CD45 has recently been studied extensively and has been suggested to have a key role in regulating an adaptive immune response [1][2]. Vital for this is the effective height of CD45 on the cell surface, which has not been accurately measured [1], [3]. We here study this on a cell membrane mimic called supported lipid bilayers (SLBs) using a range of techniques: total internal reflection fluorescence microscopy (TIRFM), fluorescence recovery after photobleaching (FRAP) and hydrodynamic trapping. These techniques are described in more detail in the next chapter. SLBs are common cell-membrane mimics that are frequently used since they provide a controlled environment to study the physicochemical properties of membrane-anchored receptors [4]. Especially the effect of salt on the orientation of the CD45 molecules on the SLB was investigated, and whether having a different salt concentration can cause the molecule to go from lying down to more upright. This would have important implications when it comes to using these systems to model real cell membranes.

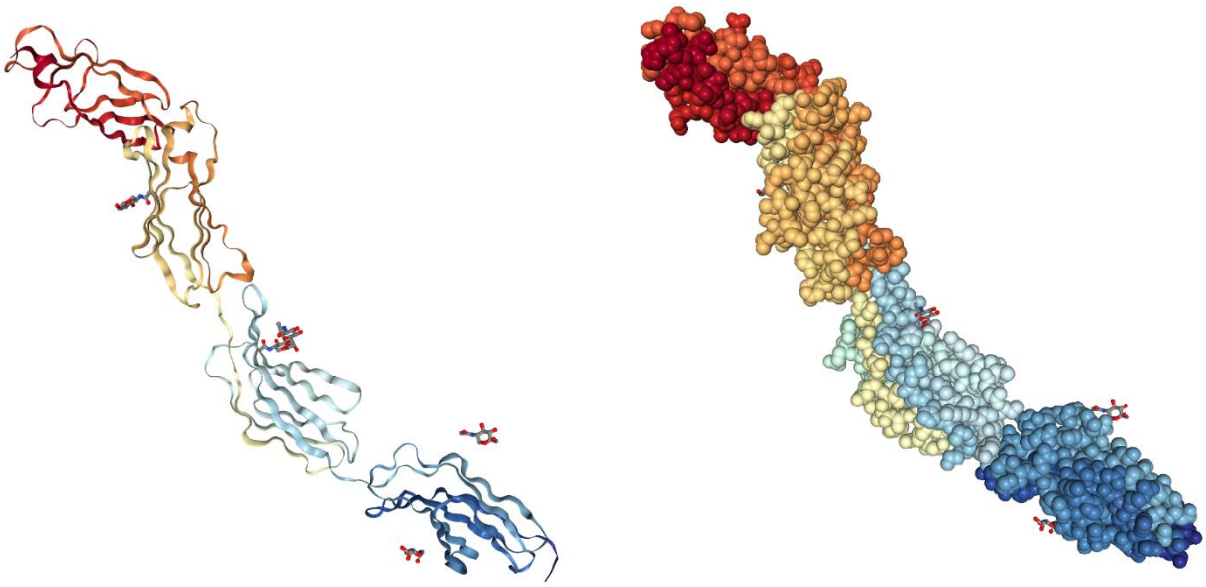

Figure 1: This is the immune cell membrane protein CD45 D1-D4. It is suggested to be responsible in the triggering of the T-cell receptor.[1]

[1] The images were produced from http://www.rcsb.org/pdb/explore/explore.do?structureId=5FMV. (Last access 2017-05-30)

2 Experimental techniques

2.1 Fluorescence microscopy

Most molecules can absorb light. Depending on the nature of the molecule, the specific wavelengths of absorbance will vary. When light of the correct wavelength hits an electron in a bond the electron may be promoted into an excited singlet state. As the electron falls back to its non-excited state, energy in the form of a photon, with a lower energy, may be emitted. This phenomenon known as fluorescence, and the time of decay for the electron to return the its ground-state lies in the timescale of nanoseconds [5].

The phenomenon of fluorescence is often taken advantage of when studying biological systems, as the reemitted photons always have a longer wavelength than the incident photon. The reason for this is that some of the energy of the incident photon is lost due to vibrations of the electron bond and eventual vibrations of the molecule, producing heat.

By using fluorophores of suitable characteristics, one can conveniently study biological systems by exciting the sample with a specific wavelength and then use a filter to highlight only the features arising from the fluorescence. The fluorophore can be native of the sample studied if the structure, for instance, possesses conjugated bonds. Alternatively, it can be added by covalently binding a fluorescent group to the studied molecule [5]. Figure 2 shows a TIRFM and how it works.

2.1.1 TIRF

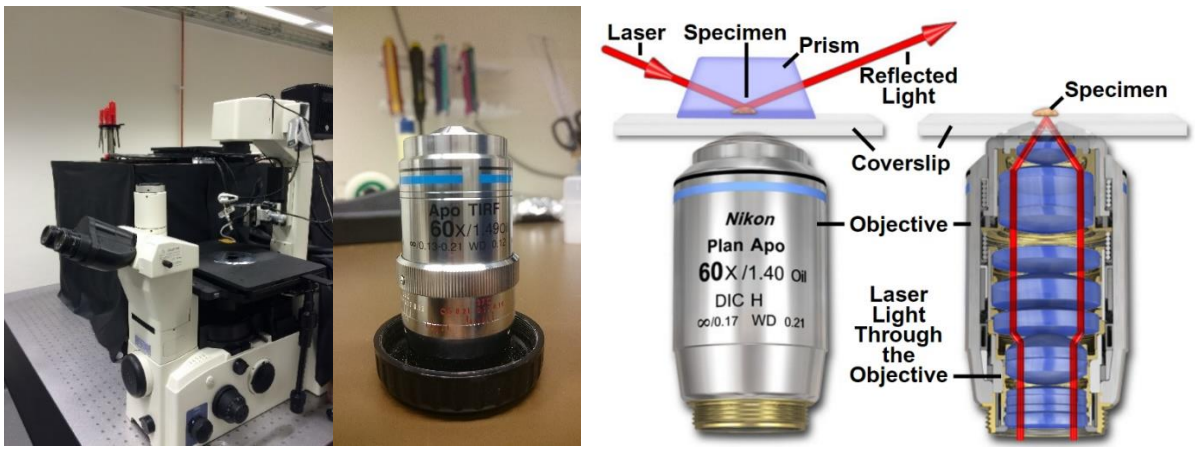

Figure 2: Left image: TIRF microscope. Middle image: The TIRF objective. Right image: Schematic over two different types of TIRF objectives. The setup of the right TIRF objective is the one used in the work. [2]

TIRF is a method that can be used to study membrane structures. The technique works by making use of the phenomena that occurs when light is totally reflected at a glass-water interface producing an evanescent wave as can be seen in Figure 2 (right image). This wave has a very small range and decays exponentially with distance (on the order of 100 nm). This is critical as you do not want all of the fluorophores in the sample to light up and preventing you from seeing the proteins in the membrane surface. With the short range of the evanescent wave,

[2] https://www.microscopyu.com/techniques/fluorescence/total-internal-reflection-fluorescence-tirf-microscopy (last access 2017-05-28)

only fluorophores close to the surface of the glass will be excited, leaving the bulk unaffected, resulting in a high signal to background ratio [5][6].

2.1.2 FRAP

A cell membrane consists of a lipid bilayer and the lipids have the ability to move across the plane, i.e. they are fluid [7]. FRAP is a method used to measure this mobility and determine the diffusion constant of labelled molecules in a medium. By continuously exposing a small area of a sample, by using an iris, to high intensity light over several seconds, the fluorophores in an area become bleached, leaving behind a dark spot as seen in Figure 3. The whole sample is then monitored at a lower light intensity and the diffusion of fluorophores into the area is determined, whether it is the fluorophore itself or a molecule in which it is connected to [5][8].

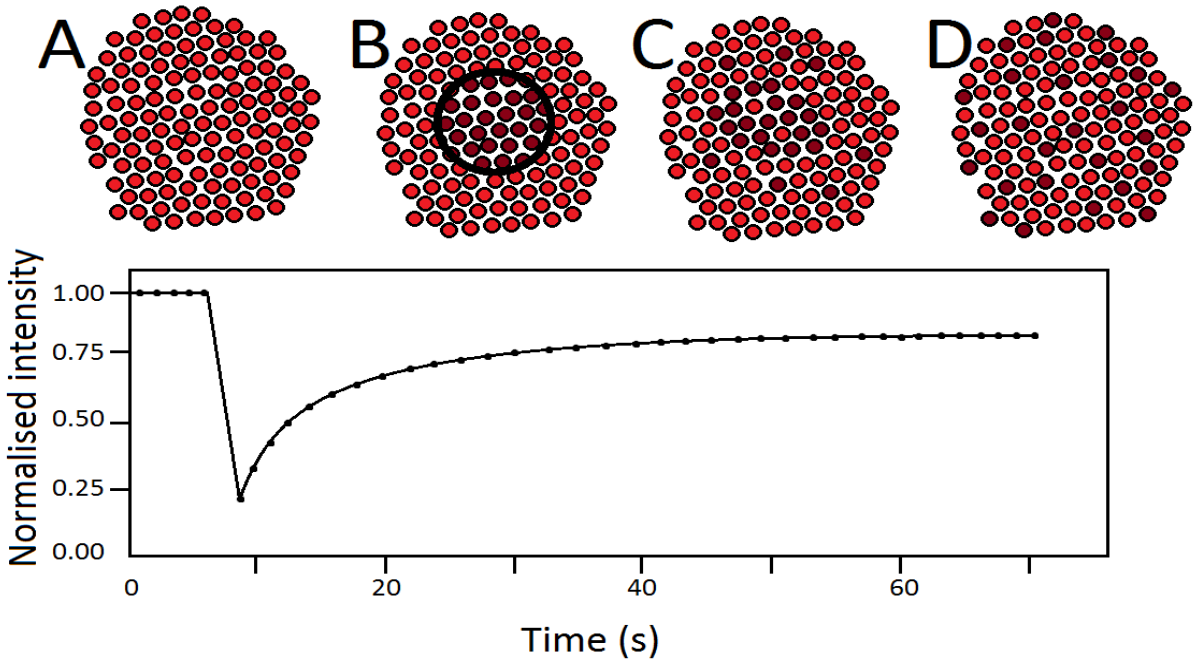

Figure 3: A schematic over FRAP. (A) The fluorophores before bleaching. (B) The encircled region is exposed to high intensity light. (C) Diffusion of the fluorophores takes place. (D) Uniform diffusion of the bleached fluorophores over the entire cell.

2.2 Hydrodynamic trapping

Many important reactions occur at the cell membrane interface. Signals are transmitted, molecules attach to receptors and proteins interacts with one another. In order to be able to study molecules, more specifically membrane proteins, we sometimes need to be able to control their motion. Currently, there are a couple of methods that allows one to manipulate molecules and study them. Optical traps [9], electric fields [10] and acoustic waves [11] are a few of the methods currently available. However, these methods have some limitations and there is no general method of trapping molecules anchored to a lipid bilayer, and with methods of today the procedure of the trapping of membrane proteins is tough. These issues are, for instance, that the size of the molecules trapped by the previous methods often lie in the range of 100-1000 nm, making it difficult to study small molecules in the around the size of 10 nm.

Hydrodynamic trapping is a trapping method that offers a non-contact method of general nature [12] and the principle behind it is shown in Figure 4. By utilising the hydrodynamic drag forces by creating a negative pressure into a conical pipette, molecules protruding from an SLB can

be trapped. The size of the pipette tip governs the size of the trap, giving a trap of a size similar to that of the pipette tip as the surface forces of the hydrodynamic trap quickly decreases with the distance from the pipette tip.

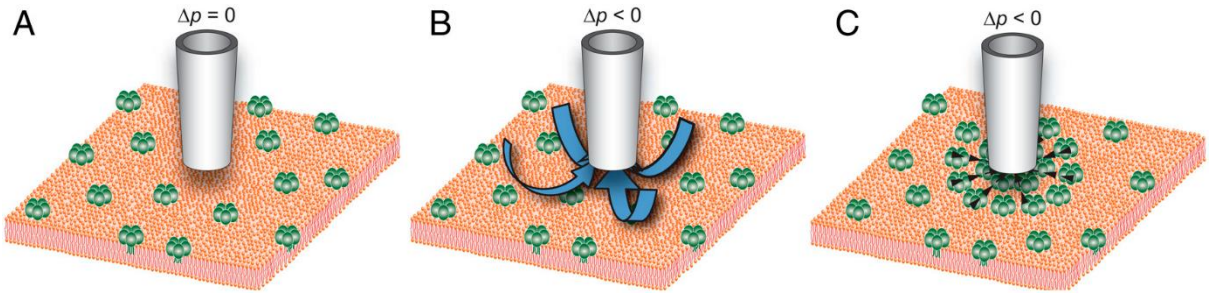

Figure 4: The principle of the hydrodynamic trap. (A) A conical pipette is lowered towards the SLB until it is approximately one tip radius above the lipid bilayer. (B) Negative hydrostatic pressure, Δp, is applied at the top of the pipette resulting in a flow of liquid into the pipette. (C) The resulting liquid flow acts on the protruding molecules in the SLB with a drag force causing them to accumulate, and become trapped, locally below the pipette. Image and description from Jönsson et al. 2012 [12].

For the hydrodynamic trap to work, it must be lowered one tip radius above the SLB. In order to get the pipette down low enough, the pipette is moved using a piezo-electric positioning system in conjunction with resistance measurement using an electrode in the pipette and one in the surrounding bath. The mechanism is the same as that of scanning ion conductance microscopy. This allows the pipette to be moved over the surface before turning on the trap over the SLB.

Once the trap is turned on, the hydrodynamic forces created by the flow of the liquid will act on the molecules. The force is greater for large molecules protruding from the SLB, causing them to gather below the pipette. Smaller molecules are affected to a much lesser extent and lipids in the bilayer that are similar to the anchored lipids can be seen as unaffected relative to protruding molecules. The reason for this is governed by how the hydrodynamic force, F_{hydro}, acts on the dimensions of the studied molecule (radius R_c; height h_c). This can be shown in the formula below [12]:

$$F_{hydro}(r) = \alpha 3\pi R_c h_c \sigma_{hydro}(r) \qquad (\mathbf{1})$$

with α being a dimensionless function depending on the shape of the molecular complexes in the SLB, R_c the effective radius and h_c the height of the molecule above the protruding part over the SLB. $\sigma_{\text{hydro}}(r)$ is the shear force per unit area on the surface of the SLB defined by [12]:

$$\alpha_{hydro}(r) = \eta \left.\frac{\partial u_r}{\partial z}\right|_{z=0} \qquad (\mathbf{2})$$

with η being the viscosity of the liquid, u_r the radial flow velocity and z the distance to the surface. An important note is that it is the liquid flow that creates the hydrodynamic trap rather than the shear force. From Eq. **1** we can see that as the molecules get bigger, R_c and h_c increase hence increasing F_{hydro}. As the largest molecules gathers first, the create a shield for the smaller molecules [12][13].

To calculate the concentration of the protein from the obtained data, the following conversion formula was used:

$$\frac{30 \cdot (mean\ gray\ value - dark\ count\ value) \cdot 100}{laser\ intensity \cdot 223} = initial\ concentration \qquad (\mathbf{3})$$

where the *mean gray value* is the mean intensity of a uniform square selection in ImageJ, *dark count value* is the intensity at the edges.

3 Materials and Method

3.1 Materials

3.1.1 Protein

The protein CD45 D1-D4 labelled with Alexa Fluor 488 (Alexa Fluor® 488 Antibody Labeling Kit, ThermoFisher Scientific, USA) was provided by the group of Prof. Simon J Davis of the University of Oxford [1].

3.2 Experimental procedure

3.2.1 Preparation of the SLB

Concentrated hydrogen peroxide (1.5 mL) was added dropwise to a beaker containing concentrated sulfuric (4.5 mL) to make a 3:1 piranha solution. The solution was then heated on a plate. A microscope cover slip measuring 25 mm in diameter was added using tweezer to the piranha solution under heating (15 min, or until bubbling ceased) to remove organic matter, and to create a better binding surface for the lipid vesicles to rupture into an SLB. Meanwhile, one well from a silicone isolator with the diameter of 4.5 mm and depth of 1.6 mm was cut (Silicone isolators, 12x4.5 mm diameter, 1.7 mm depth; Grace Biolabs). It was then cleaned with ethanol, Milli-Q water (Millipore, USA) and dried using a tissue. Tissue paper was removed from the silicone well through adhesion using tape on both sides three times. The silicone piece was stored in a petri dish with tape over it and the petri dish was covered using aluminium to prevent dust falling in. The coverslip was removed from the piranha solution and placed in a beaker of deionised water, and then rinsed thoroughly with deionised water from the tap whilst being held in tweezers, and dried using nitrogen gas. The dried coverslip was then placed and pressed gently onto the well, which attached through adhesion. The coverslip was then secured into a circular metal coverslip holder. An Eppendorf tube was filled through a filter with a buffer solution consisting of 150 mM NaCl and 10 mM HEPES (bilayer buffer). The solution was adjusted to a pH of 7.4 using a 1 M NaOH solution. 27 µL of the bilayer buffer was added to the coverslip holder and another 27 µL into an Eppendorf tube. 3 µL of a mixture of 5% DGS-NTA and 95% POPC (Avanti Polar Lipids) was added to the Eppendorf tube and mixed by pipetting up and down. The resulting 30 µL mix was added into the bilayer buffer in the coverslip holder and left for 1 hour for the vesicles to form the SLB. The buffer of interest (BOI) was filtered into an Eppendorf tube. The SLB was washed 5 times with a pipette set at 40 µL using the BOI and pipetting the solution 3-4 times. CD45 was diluted 1:100 by adding 1 µL of CD45 to 99 µL BOI in an Eppendorf tube. 28.5 µL BOI was added to an Eppendorf tube followed by 1.5 µL of the diluted CD45. The resulting 30 µL sample was loaded onto the SLB. The protein was left to anchor into the SLB over 1 hour.

3.2.2 Microscope setup

An inverted Nikon Eclipse TE2000-U microscope (Nikon Corporation, Tokyo, Japan) was used to observe the intensities of the labelled CD45. A solid-state laser (Cobolt AB, Sweden) was used to illuminate the sample, operating at 488 nm. The images were acquired using an ORCA-Flash4.0 LT SCMOS camera (Model C11440-42U, Hamamatsu, Japan) which was attached to a W-VIEW GEMINI beam splitter (Model A12801-01, Hamamatsu, Japan). The two objectives used (Nikon instruments, Japan) for measuring the pipette was a CFI S Fluor 20X objective (NA=0.75) and for the FRAP runs and the trapping a CFI Apo TIRF 60X Oil objective

(NA=1.49). The microscope was managed through the program MicroManager (μManager) [14].

3.2.3 Running the FRAP

The FRAP was ran using a 488 nm laser to illuminate the CD45 couple with Alexa Fluor 488 at an intensity of 60 mW. A script called *Vicky_FRAP* was used. It took a total of 60 frames at an interval of 2 s between frames. Before the 5^{th} frame, a flip-mounted shutter (Thorlabs, Newton, USA) was lowered to bleach only a small region of the sample. The region was then bleached with high-intensity laser for a few seconds. After the 6^{th} frame the shutter was lifted, the laser was attenuated and the recovery of the proteins on the SLB monitored.

3.2.4 Pipette pulling and Hydrodynamic Trapping

The micropipettes were pulled (Figure 5) using a flaming/brown micropipette puller (Model P-97; Sutter Instrument, USA) using Borosilicate Glass Capillaries (item number 1B100F-4, World Precision Instruments, USA) and the blunt end was flamed to make it less sharp when fitting it to the custom-made pipette holder on the microscope. An electrode attached to the pipette holder was placed in bleach for 15 minutes to re-activate it. The pipette, filled with the BOI, was mounted onto the custom-made holder which in turn was attached to a piezoelectric three-dimensional positioning system allowing for sub-100 nm in three dimensions. The pipette was lowered into the coverslip holder, which had been filled with 1 mL BOI to create an electrode bath and a circuit, until it was seen with the TIRF objective and the tip was focused carefully, Figure 6. The pipette tip was centred and then brought down closer to the SLB surface using the piezoelectric positioning system. A resistance meter was used to monitor the lowering, which was until a rapid increase in resistance was registered. Upon this the pipette was moved back 2 μm. A stepper motor was used to control the position of a 10 mL syringe, creating hydrostatic pressure at the top of the pipette. By using a custom-written program in LabVIEW 2009 and a custom-made pressure sensor, the pressure was monitored and feedback sent to stepper motor in order to maintain the pressure [12]. Negative pressures between 3 and 20 kPa were used and the data saved as TIFF-files for further analysis.

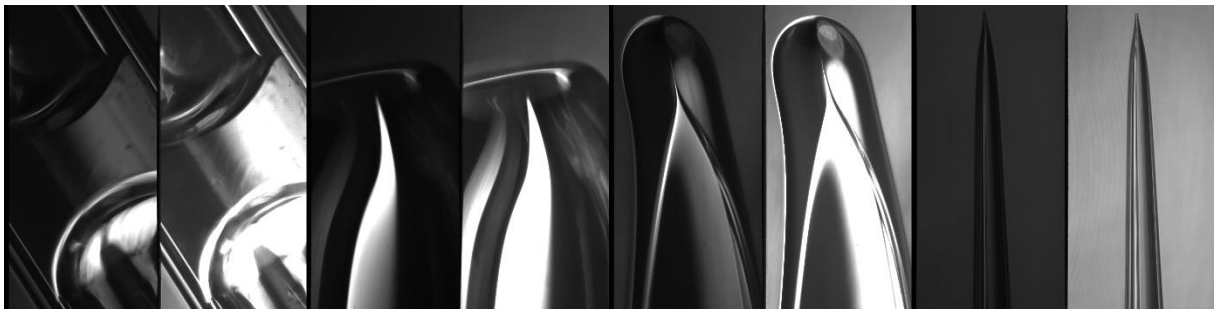

Figure 5: Making the perfect micropipette. The images here are all glass capillaries that can become micropipettes. The one furthest to the right was pulled using the flaming/brown micropipette puller and the image taken using the 20x objective, whilst the other are just flamed.

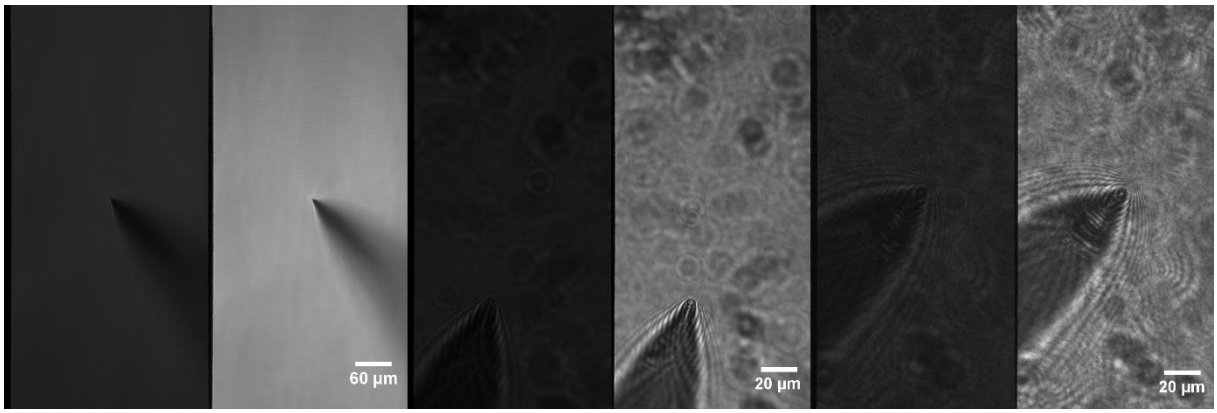

Figure 6: Approaching the lens with the micropipette. The left image: Approaching the lens using the 20x objective. The middle and right images: Approaching the pipette with the 60x TIRF objective. Here, the pipette has to be lowered using the piezoelectric positioning system and the resistance.

3.2.5 Programs for analysing the data

For data analysis, four programs written in MATLAB, previously written by my supervisor Peter Jönsson, were used.

The FRAP data was analysed using a program called *frap_analysis*. It analyses images saved in TIFF-format and was used to measure the diffusion constant of CD45 in the SLB and the immobile fraction [15].

For the analysis of data gained from the hydrodynamic trapping a program named *accumulation* was used that measured A_{hydro}-parameter [13]. For this, the pipette dimensions and the concentration needed to be calculated first. The dimensions were calculated using the program ImageJ and the protein concentration was calculated using ImageJ and MS Excel using the conversion formula from Eq **3** in section 2.2. The data for the hydrodynamic traps at the different pressures could then be obtained.

The data obtained from the A_{hydro}-curves were then taken and plotted in one graph, saved, and the resulting plot was further analysed with the program *Average_interaction*, were the mean value of the lines in the same domain was calculated.

The resulting plot was saved and then used in a program called *TrapFit2_new*. The height of the proteins protruding over the SLB were obtained by manually fitting a curve to the plot obtained from the previously mentioned *Average_interaction* program.

4 Results and Discussion

In this chapter, the obtained results are discussed. For convenience, the buffer solutions will only be referred to as 10 mM NaCl, 10 mM buffer solution etc. The HEPES concentration is always present in all samples at the concentration of 10 mM.

4.1 Diffusion

A total of 15 experiments were conducted with 14 of them yielding data. In Table 1, the diffusion for CD45 of the experiment are shown, excluding data from the two FRAP tests were the diffusion at different salt concentrations were made.

Table 1: Here, FRAP data from some of the experiments are presented. The buffer contained 10 mM HEPES, the diffusion concerns CD45 mobility through the SLB, and k_{max} gives size of the data set used for fitting.

Buffer NaCl conc.	Experiment	Diffusion constant [$\mu m^2 s^{-1}$]	Immobile fraction %	k_max
150 mM	001	1.0103	64	0.023612
	002	1.3805	16	0.025268
	Mean	1.1954		
	St.dev.	0.2618		
500 mM	003	0.94998	5.1	0.028505
	005	1.0048	1.1	0.036249
	007	1.1607	2.8	0.035356
	008	1.1315	0.53	0.035051
	009	-	-	-
	010	1.233	13	0.026935
	011	0.92368	11	0.034425
	012	1.031	0.80	0.034584
	013	1.0236	2.9	0.028201
	Mean value	1.0573		
	St.dev.	0.1076		
10 mM	014	1.2317	0.2	0.02865
	015	1.6524	3.7	0.029136
	Mean	1.44205		
	St.dev.	0.2975		

From Figure 7, in which the data from Table 1 have been used, the 10 mM NaCl buffer solution seems to have the highest diffusion constant followed by the 150 mM buffer and lastly the 500 mM solution. When considering the standard deviation however, the mean diffusion of CD45 in the 10 mM buffer lies in the same range as the 150 mM buffer and close to that of the 500 mM. When looking at Figure 10-11 and Figure 14-15, we see that there is no trend in with increasing salt concentration (more discussion on the images will come in the next section). It is most probable that the diffusion is similar for the different concentrations. The reason why the 500 mM buffer has a smaller diffusion could probably be that its data set is larger. Another reason for the difference is that each SLB is a little different from one another and there will therefore be differences in quality and attributes. An important thing to consider is the bleached region. When conduction some of the early experiments, the shutter used to narrow in on a region to bleach was not functioning properly and the shutter had to be manually opened and

closed. This caused the size of the bleached area to differ mainly for the early experiments. For the later ones, the flip mount worked, allowing for the bleaching region to be the same for each FRAP as the shutter size was no longer altered manually. A while later, there was again issues with the flip-mount and it had to be manually moved down. This time, however, the size of the opening of shutter wasn't changed in order to carry out the bleaching. The poor diffusion and large bleaching area of the SLB from experiment 001 compared to experiment 002 can be seen in Figure 8 and Figure 9 respectively. This, along with vibrations from inside and outside of the room, plus sliding of the sampler holder, could be the reason for which the diffusion from Figure 7 looks the way it does compared to that of Figure 10-11 and Figure 14.

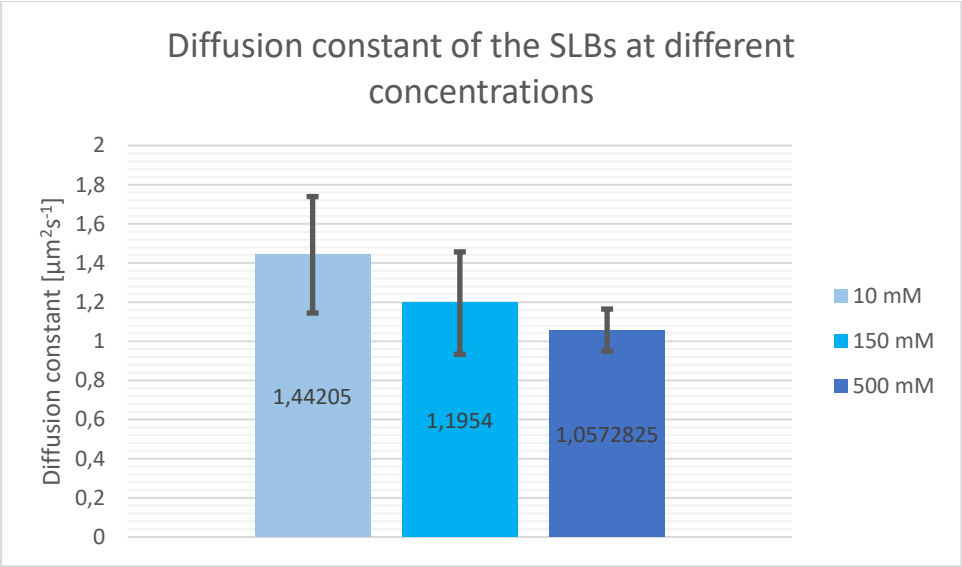

Figure 7: Here, the obtained diffusion constants from the different experiments have been displayed.

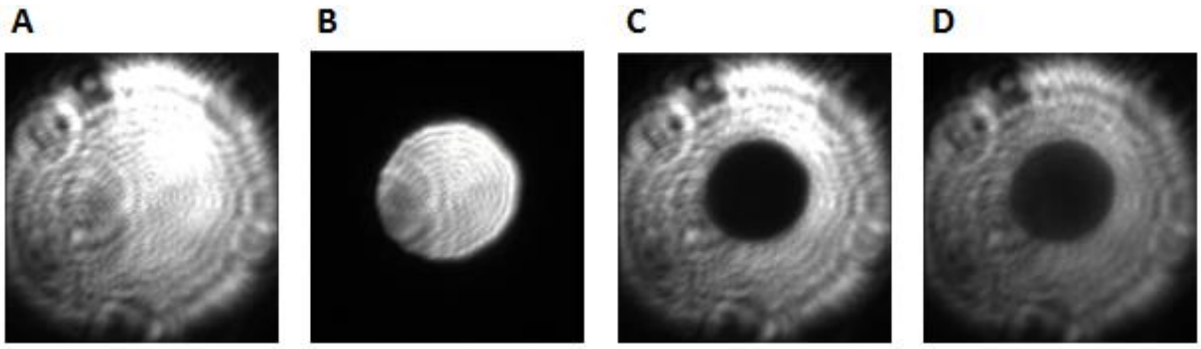

Figure 8: The resulting FRAP of experiment 001. (A) This is the 1st frame before any bleaching has occurred. (B) The shutter is closed and the laser set to an intensity of 60 bleaches the spot. (C) This is the 7th frame after the bleaching has taken place. (D) At the 60th frame few lipids have diffused into the bleached spot signifying a poor diffusion, hence SLB.

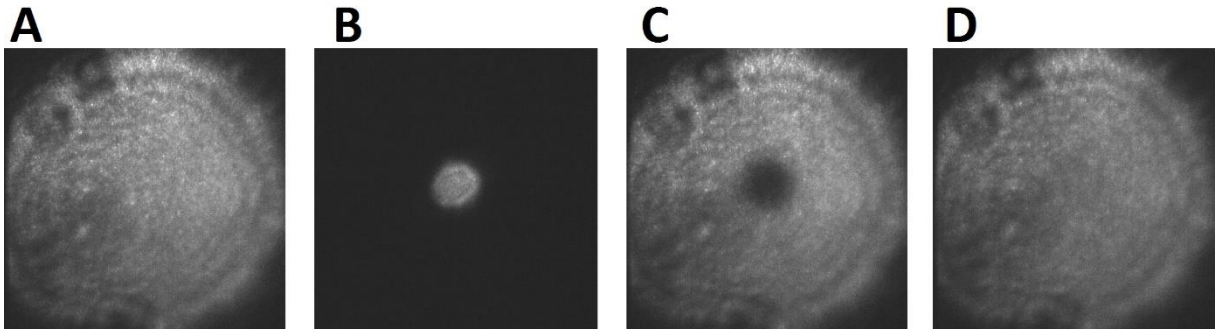

Figure 9: The resulting FRAP of experiment 002. (A) This is the 1st frame before any bleaching has occurred. (B) The shutter is closed and the laser set to an intensity of 60 bleaches the spot. (C) This is the 7th frame after the bleaching has taken place. (D) At the 60th frame we can see that the SLB has recovered.

4.1.1 FRAP tests on different salt concentrations

An experiment was made on an SLB with CD45 where the diffusivity was measured for different buffer solutions. The buffer was thus changed after each measurement after careful rinsing. The diffusivity of CD45 for the different cases is shown in Table 2. Figure 10 shows the diffusivity in a plot as a function of salt concentration whereas Figure 11 shows it as a function of when the FRAP experiment was made. Figure 12 and 13 shows the immobile fraction of CD45, and are a part of experiment 004.

Table 2: Data from experiment 004. These are the results obtained for the SLB after running the FRAP. The two yellow fields are reruns made after the 75 mM NaCl run. These were made due to detected data overwriting.

NaCl conc. [mM]	Diffusion constant [$\mu m^2 s^{-1}$]	Immobile fraction	Percent	k_{max} [μm^{-1}]
10	1.1318	0.11079	11	0.027229
10	0.92235	0.16861	16	0.027205
15	0.95763	0.23083	23	0.027463
30	0.81982	0.1384	13	0.030177
30	0.85319	0.14253	14	0.026951
50	0.87354	0.14699	14	0.028201
50	1.0296	0.063498	6.3	0.02768
75	0.90846	0.097026	9.7	0.027698
Mean value	0.93704	0.137334	13	0.027826
St.dev.	0.10195	0.050174	4.9	0.001024

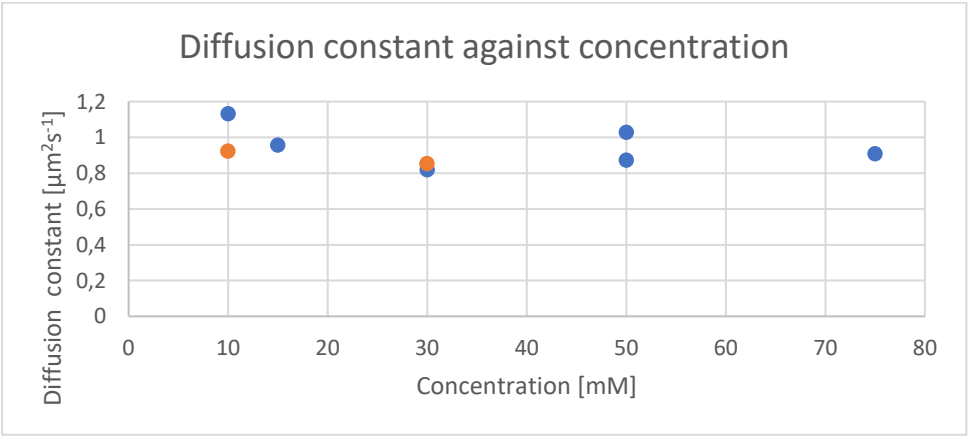

Figure 10: In this figure, the diffusion constant has been plotted against the concentration. The orange dots are reruns made after the 75 mM run. There is no significant jump in diffusion concentration when going up in concentration.

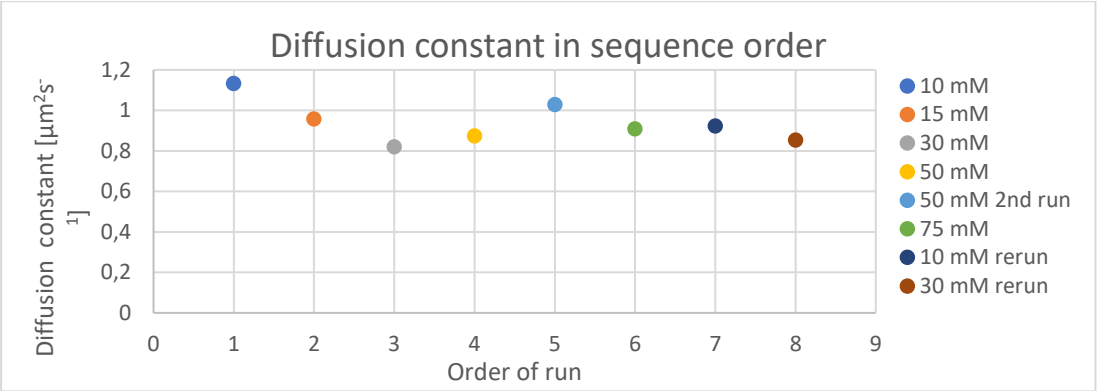

Figure 11: Here the diffusion has been placed in the order in which the FRAP was carried out.

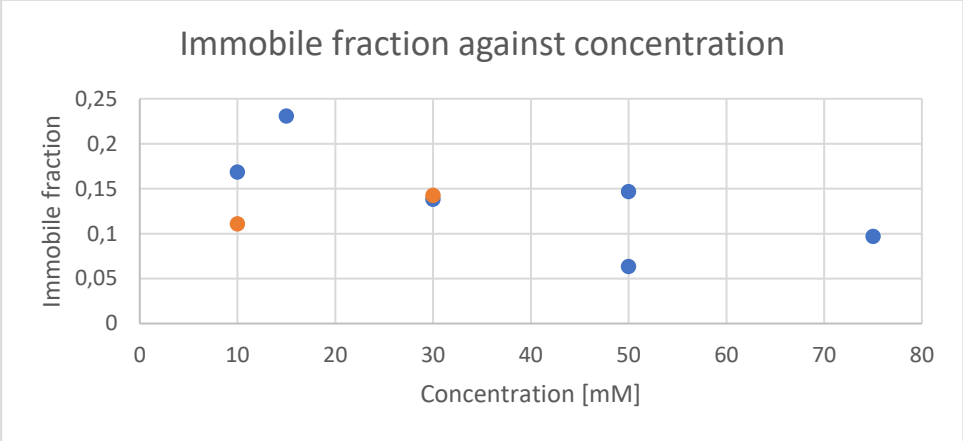

Figure 12: The mobility of the lipids as the concentration increases have been plotted here with the orange dots being reruns med after having made the 75 mM run.

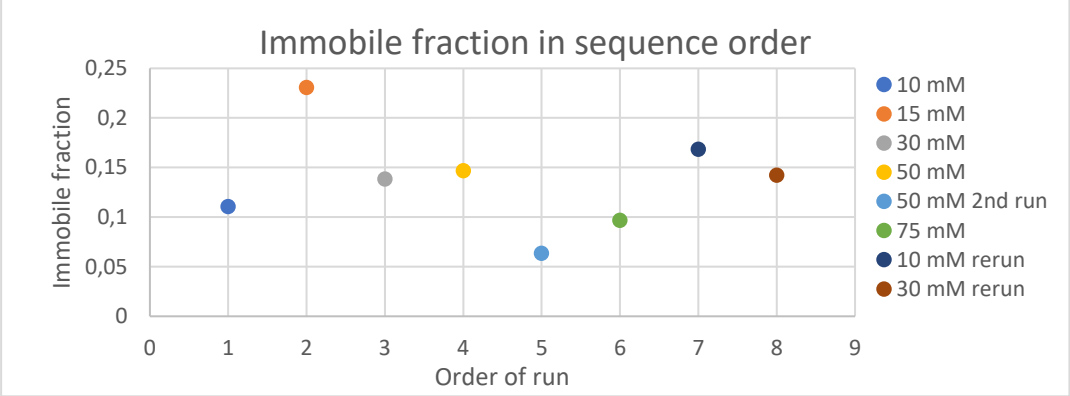

Figure 13: The immobile fraction in the order of the time at which each run was carried out.

From Table 2, the mean diffusivity was 0.9 ± 0.1 $\mu m^2 s^{-1}$ and the mean immobile fraction was 0.13 ± 0.5, or 13 ± 5 %. When it comes to the immobile fraction, no pattern could be observed from Figure 12 nor Figure 13. A second experiment was conducted, including a 150 mM NaCl standard and a 500 mM NaCl sample, in order to see if a trend could be found that might not have visible due the poor experimental procedure and relatively low salt concentrations.

Below, the second diffusivity test, experiment 006 is discussed. This experiment was carried out similar to the aforementioned experiment 004, with the difference being that the bilayer was allowed to incubate for 5 minutes between each run. The diffusivity of CD45 for the different cases is shown in Table 3. Figure 14 shows the diffusivity in a plot as a function of salt concentration. Figure 15 shows the immobile fraction of CD45.

Table 3: These are the results obtained for the diffusion of the SLB after running the FRAP. During the shaded 75 mM NaCl run the sample holder started to slide, causing the frames after number 30 to be useless. For the 500 mM NaCl run a rerun was made due to not having let it incubate for the minimum 5 minutes. The two data values have been excluded for the calculation of the mean value and standard deviation.

NaCl conc. [mM]	Diffusion constant [$\mu m^2 s^{-1}$]	Immobile fraction	Percent	k_{max} [μm^{-1}]
10	1.075	0.052452	5.2	0.031061
15	1.1287	0.017448	1.7	0.029214
30	1.1027	0.040898	4.0	0.025251
50	0.94624	0.079668	7.9	0.028551
75	0.83506	0.10152	10	0.029647
75	1.2425	0.061943	6.1	0.028413
150	0.88348	0.078104	7.8	0.028138
500	0.75489	0.039307	3.9	0.02711
500	1.162	0.075225	7.5	0.028665
Mean value	1.07723	0.057962	5.7	0.028470
St.dev.	0.124164	0.022926	2.3	0.001721

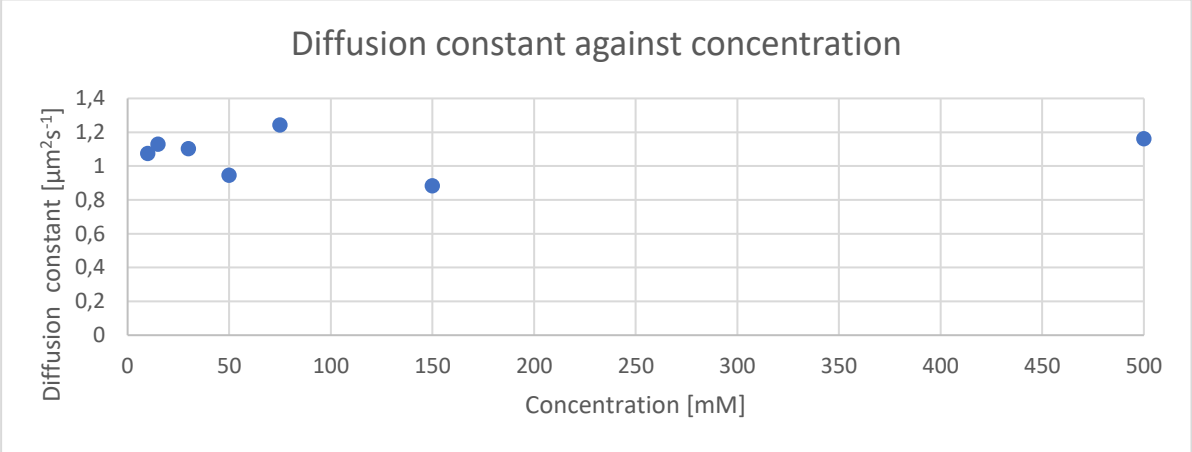

Figure 14: Here the diffusion constants have been plotted excluding the 75 mM NaCl buffer that slid and the 500 mM NaCl buffer that wasn't incubation for a minimum of 5 minutes.

When it comes to the diffusion of CD45 in different salt concentrations, no significant difference can be seen in Figure 14. The mean diffusion constant was 1.1 ± 0.1 $\mu m^2 s^{-1}$. When looking at Figure 15, it appears that the salt concentrations which contain 50 mM NaCl or more have a larger immobile fraction compared to the ones of lower concentrations, with the 50, 150 and 500 mM having nearly the same immobile fractions but it is most likely random as the mean value was 0.06 ± 0.02, or 6 ± 2 %. It can however be concluded that experiment 006 was an improvement over the previous one as the standard deviations were lower the second time around. Letting the SLB incubate for a minimum of 5 minutes also seem to play an important role as can be seen by comparing the two 500 mM FRAP tests in Table 3.

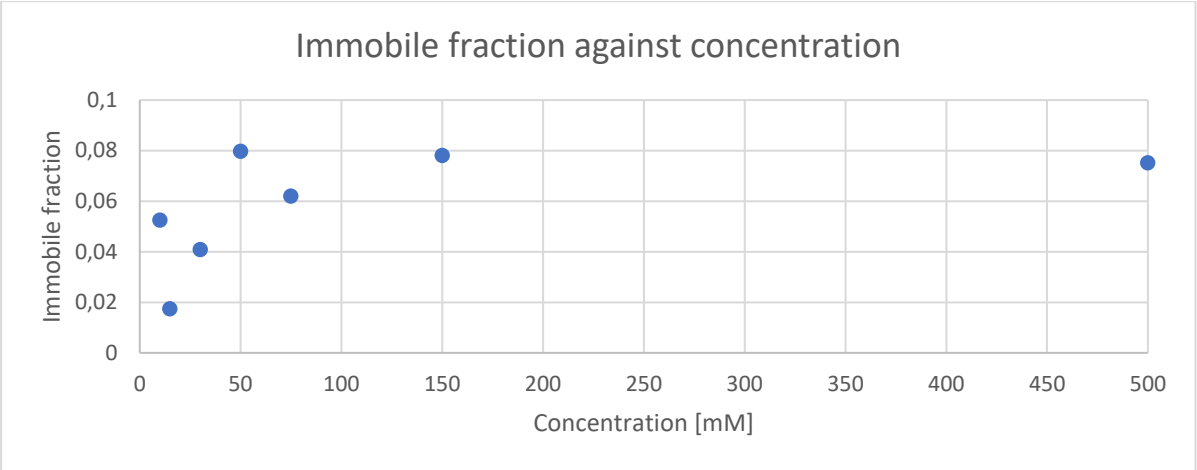

Figure 15: Here, the immobile fraction as a function of NaCl concentration in the buffer solution has been plotted. The 75 mM run in which the coverslip slid and the 500 mM with no incubation have been omitted.

In Figure 16, a set from the hydrodynamic trapping of experiment 002 is shown.

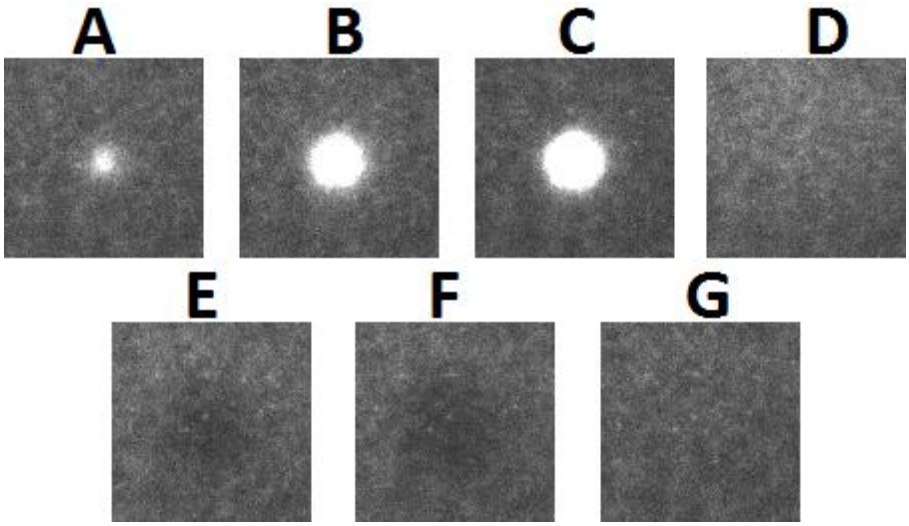

Figure 16: Trap II. (A) -2.7 kPa, (B) -9.5 kPa, (C) -19.2 kPa, (D) spontaneous release, (E) +10 kPa, (F) +20 kPa, (G) release.

In Figure 17, the sliding from the 75 mM NaCl run of experiment 006 is shown and the result is a dataset of low quality.

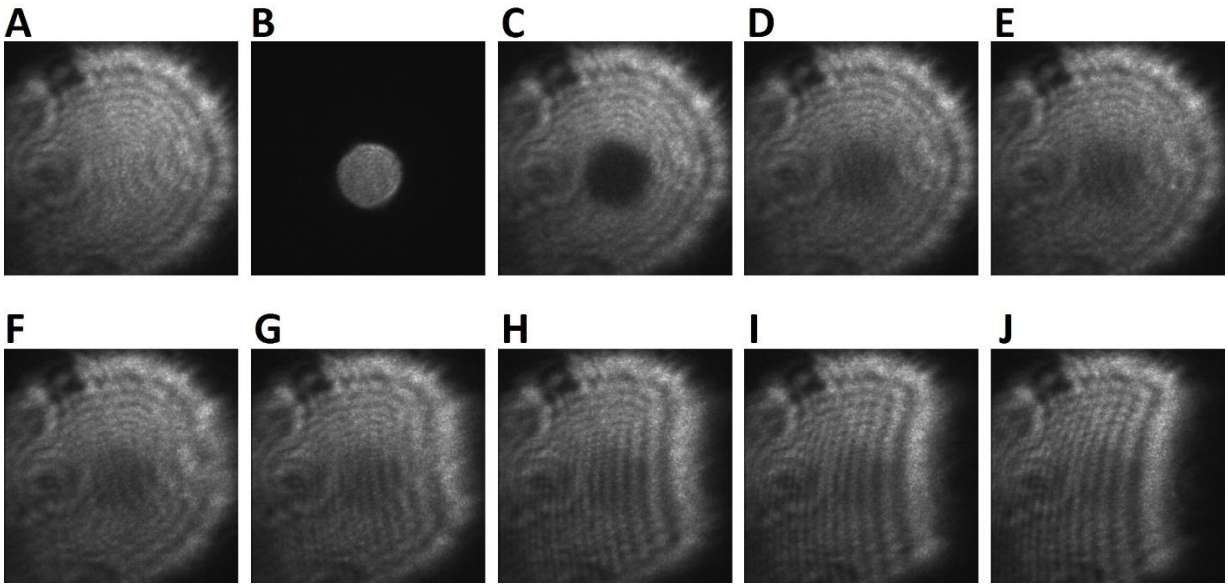

Figure 17: The sliding of the cover slip while doing FRAP of the 75 mM NaCl buffer. (A) This is the 1st frame before any bleaching has occurred. (B) The shutter is closed and the laser set to an intensity of 60 bleaches the spot. (C) This is the 7th frame after the bleaching has taken place. (D) At the 30th frame we can see that the SLB has recovered a lot. Afterwards, the coverslip starts to slide over the immersion oil causing the ripples seen from E-J. (E) 35th frame. (F) 40th frame. (G) 45th frame. (H) 50th frame. (I) 55th frame. (J) 60th frame.

4.2 Hydrodynamic Trapping

In Table 4, the obtained data from the hydrodynamic trap experiments on CD45 are displayed. Figure 18 shows the resulting height of the CD45 protruding over the SLB. The blank lines in Table 4 are those in which no data was obtained due problems that were encountered which will be discussed later on.

Table 4: Data of the proteins height above the SLB, obtained from fitting the curves from the accumulation program (section 3.2.5.) and using Tripfit2_new (section 3.2.5).

NaCl conc.	Experiment	Height [nm] $\alpha_{end} = 5$	A_{hydro} [nm^2]	Height [nm] α_{end} is varied	A_{hydro} [nm^2]	Tip diameter [µM]
150 mM	001	4.00	133.9889	4.55	156.5507	3.028
	002	4.153	140.1452	4.153	140.1452	3.227
	Mean value	4.076	-	4.351	-	-
	St.dev.	0.1082	-	0.2806	-	-
500 mM	003	5.45	196.1347	-	196.1347	4.968
	005	N/A	N/A	N/A	N/A	N/A
	007	11.25	530.5855	-	530.5855	1.32
	008	-	-	-	-	-
	009	-	-	-	-	-
	010	-	-	-	-	-
	011	4.700	162.9525	5.85	214.7895	3.888
	012	6.629	253.0192	11.38	539.6911	2.281
	013	10.5	479.6034	10.28	465.0844	2.484
	Mean value	7.706		8.886		
	St.dev.	2.985		2.9765		
10 mM	014	-	-	-	-	-
	015	-	-	-	-	-

On average, the CD45 was shown to be protruding 4.1 ± 0.1 nm over the SLB when in the 150 mM NaCl buffer and 8 ± 3 nm when in the 500 mM buffer and using a set a_{end} (a_{end} is a parameter used to fit the curve the program *Trapfit2_new*) and only fitting the initial curve obtained in *Trapfit2_new*. When the plots obtained were fitted by varying a_{end}, the height above the SLB for the 150 and 500 mM buffers were 4.4 ± 0.3 nm and 9 ± 3 nm. In Figure 18, the results are plotted along with the standard deviation. When the plots were fitted by varying the parameter a_{end}, the difference between the two 500 mM samples was more than 1.1 nm which is a significant difference.

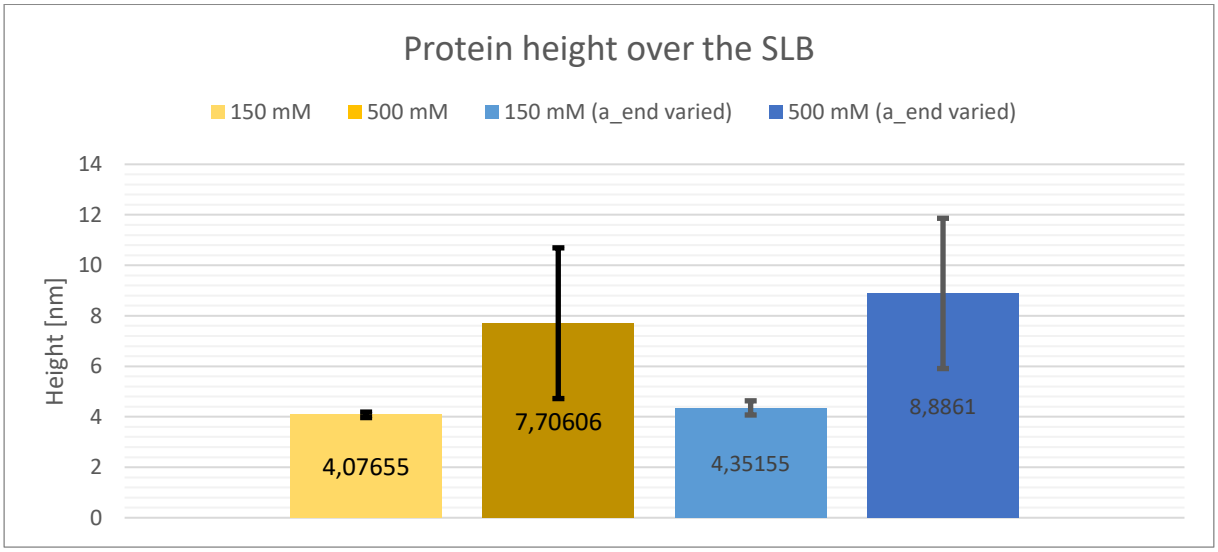

Figure 18: The obtained height of the proteins at the different concentrations with a fixed a_{end} and with a_{end} varied.

4.3 Encountered problems

Many problems were encountered when running the experiments without a high enough skillset. Lowering the pipette took a lot of time at first and quite a few runs were ended early due to lowering the micropipette for to low and contacting the glass.

Another problem that was often encountered was the clogging of the pipette, which happened quite a few times which are displayed in Figure 19 and 20.

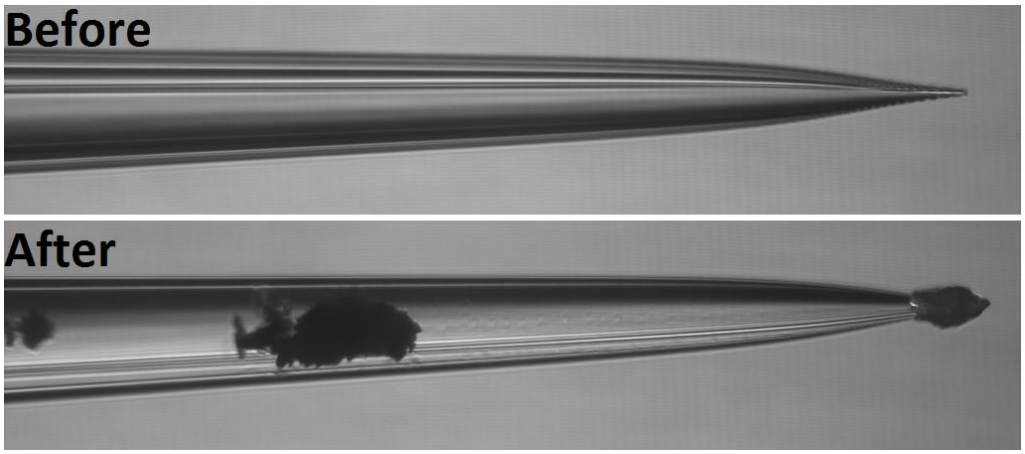

Figure 19: Here we can see in the after-image that there is some residue that has formed. It is assumed to be salt crystals of sodium chloride.

As can be seen in figure 20, crystallisation on the tip is taking place. To counter this issue, the tip was lowered into the solution as early as possible. This took place over the timescale of a few minutes of having the pipette out in the air and was observed using the 20x objective.

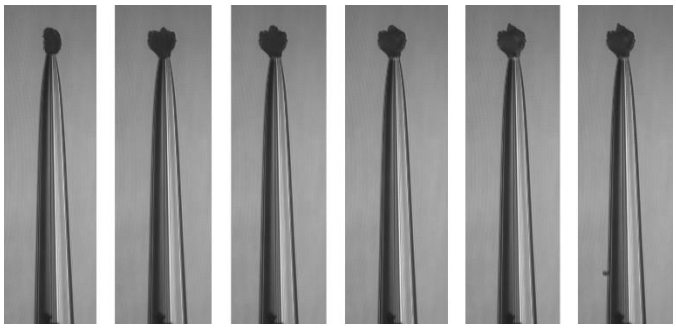

Figure 20: The formation of salt on the tip over time.

An attempt to wash the pipette tip in Figure 20 was made and it was revealed that the tip of the pipette was still intact. However, there were several particles in the pipette and none of the methods I tried to use helped to in making the pipette usable for trapping as seen in Figure 21.

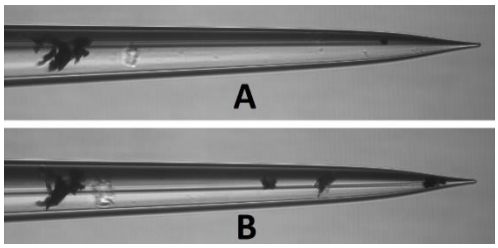

Figure 21: These images are taken after having attempted to trap. (A) The pipette tip was dipped in Milli-Q water, revealing that the tip was still intact. (B) The result of trying to dissolve particles with Milli-Q water.

In experiment 013, the blocking was further up in the pipette as can be seen in Figure 22, and caused the resistance to rise quickly until giving an O.L reading.

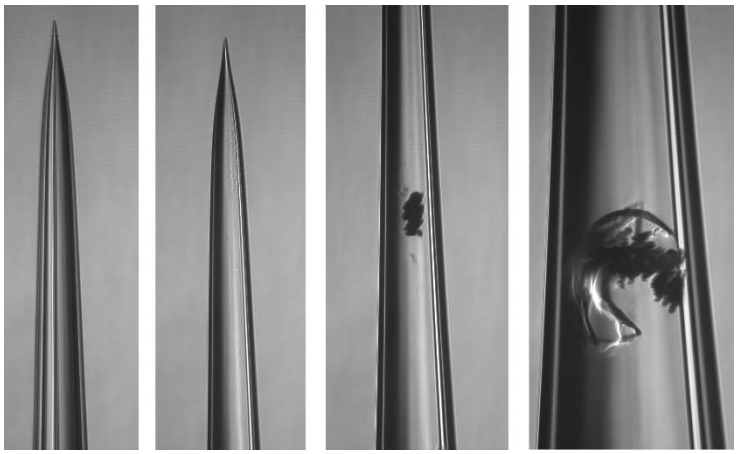

Figure 22: Here we can see a large particle blocking the pipette. This is most certainly the cause of the rapid increase in resistance that was noticed during the experiment.

Further analysis of the Trap is carried out using MATLAB-programs. In Figure 23, all the curves from experiment 013 were placed in one plot. From Figure 23 we can see the effects of a spontaneous release when observing the orange and black lines. The orange line at a pressure of 2.9 kPa has a much smaller gradient then its red counterparts. The solid black line is right before the spontaneous release. It isn't as affected as the orange line but you can see how it deviates towards the end as the radiant exposure increases. Neither the orange or black curves were used for the *Trapfit2_new* due to influence of the spontaneous release. In Figure 24 and 25 screenshots of the *Trapfit2_new* are displayed.

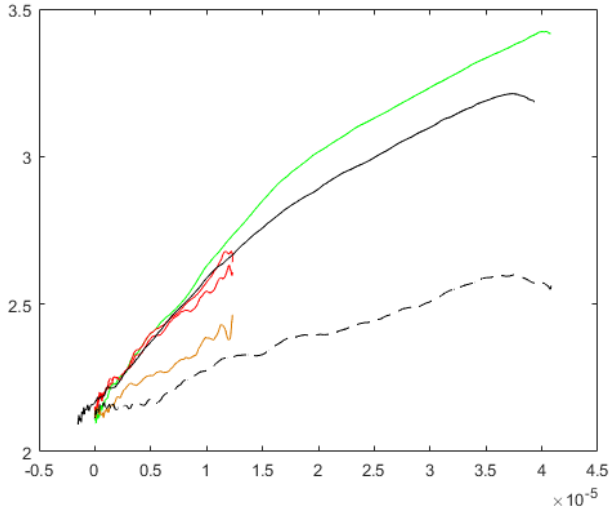

Figure 23: Here, the plots of ϵ_{hydro} from all the hydrodynamic traps at different pressures are placed into one graph. The red lines are from the pressure of -2.9 kPa, and the green one is -9.6 kPa. The two black lines are from the 2nd trap at -9.6 kPa. The solid black line is before the spontaneous release and the dashed line is right after the spontaneous release. The orange line is also a set of the 2nd trap. The height obtained from TrapFit2 was 10.5 nm and the $Ahydro_0$ was 479.6034 nm^2.

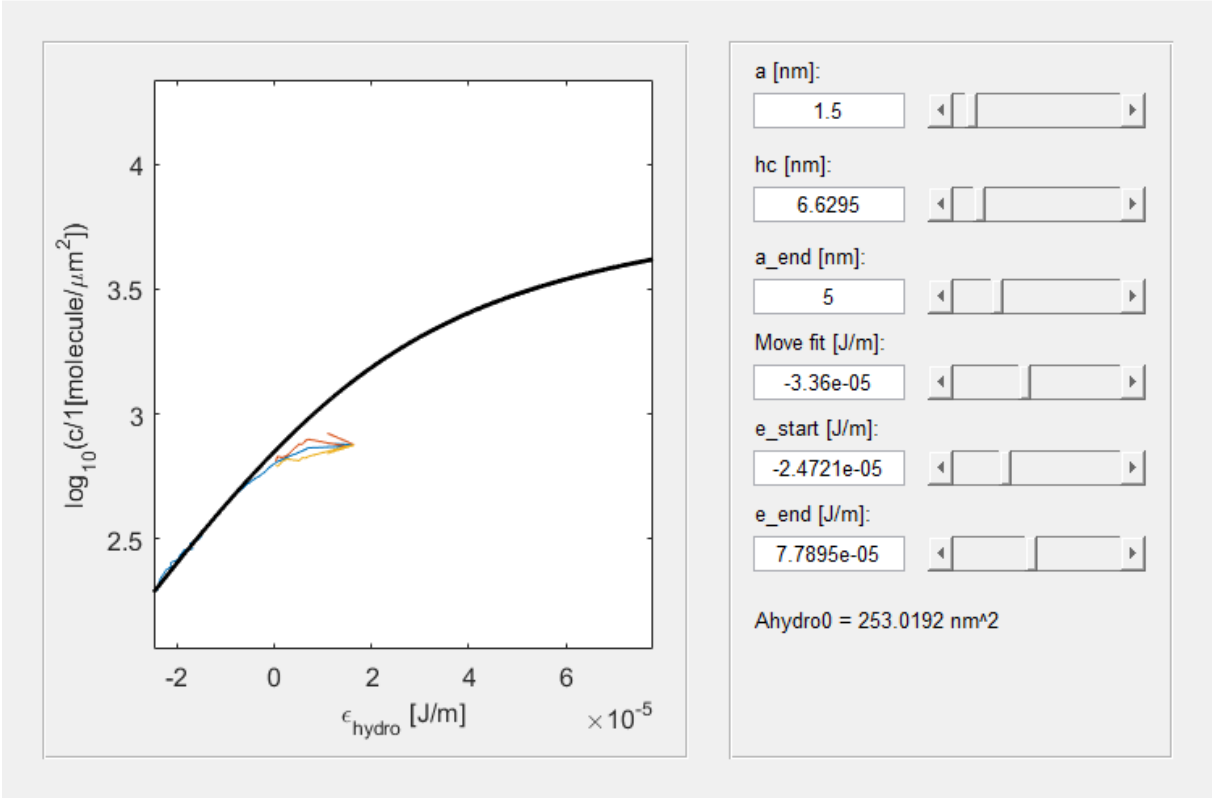

Figure 24: Regular fit with unchanged a_{end} giving a height of 6.6 nm.

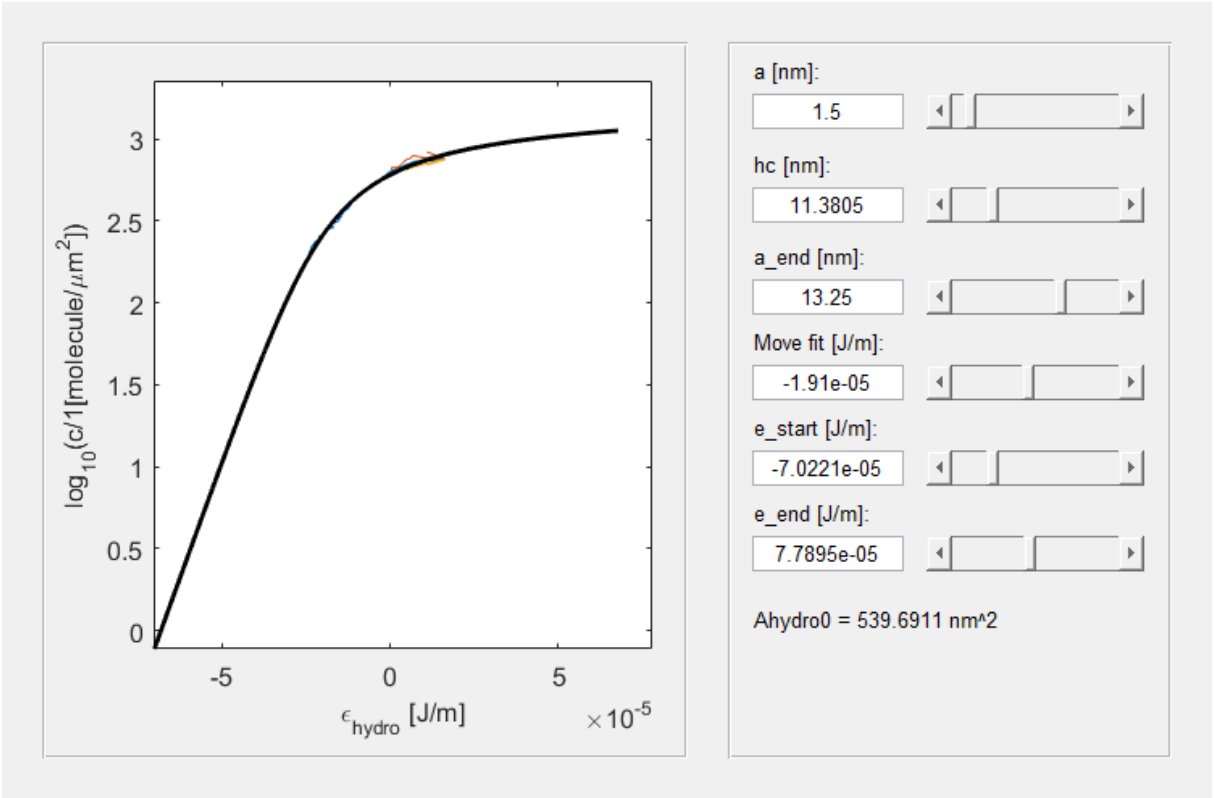

Figure 25: Here the data has been plotted with extra accuracy giving a height of 11.3805 nm

In experiment 014, the trapping didn't work at all due to issues with the resistance meter which only gave O.L. outputs. Another pipette that was available was used but, unfortunately, it got clogged as well as can be seen in Figure 26. The resistance meter was tested in water and some of the available buffer solutions and it seemed to work well.

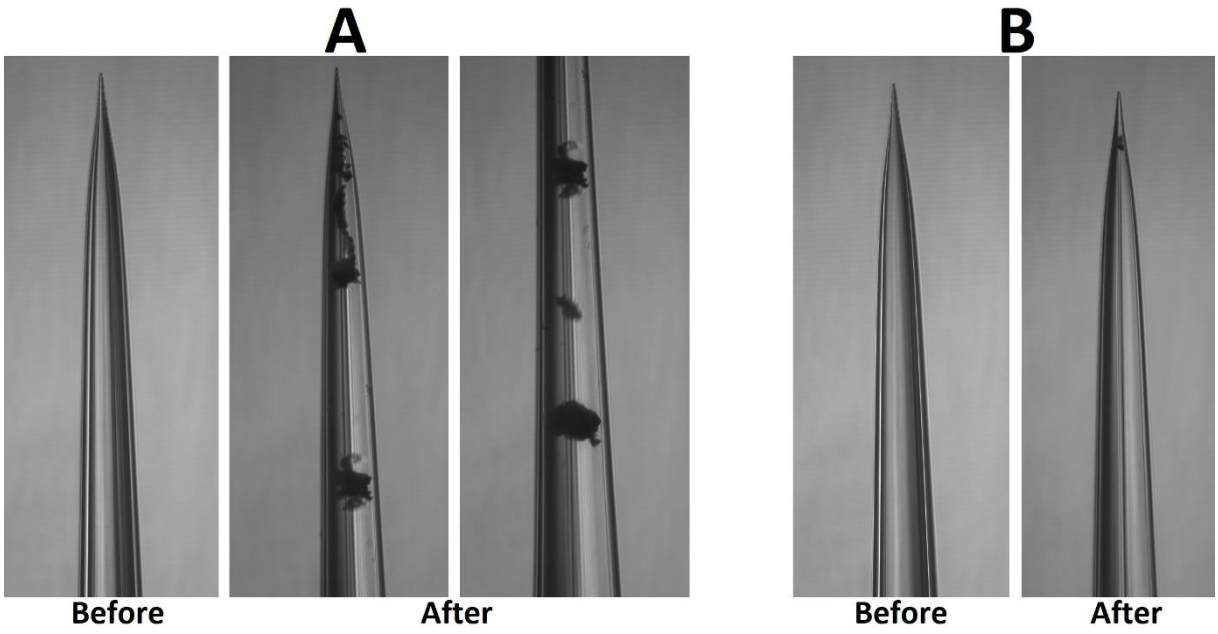

Figure 26: (A) This was the pipette that was first used. Major blockage is visible in the pipette in the image taken afterwards with major pieces further down. (B) In the second pipette a small particle can be seen blocking the tip in the image after having added the pipette.

For experiment 015, no blockage was visible in the pipette (Figure 27B). The conclusion was drawn that the issue must then come from the piezo electrode. The electrode was bleached for 15 minutes every time before it was used to remove eventual dirt but this might also have been a potential source of the issues that occurred with the resistance. As the electrode is bleached, chloride ions react with the surface of the electrode creating a layer over time that is unable to conduct. As a result, the bleached part of the electrode is unable to register any resistance.

It was checked if this was the case using the resistance meter. From Figure 28 the suspicion was confirmed. The upper, unbleached, part still worked, having only a very low resistance but the lower part gave an O.L. reading, as seen in Figure 28. Since it had been working during the previous experiment it was never given much thought, especially since the pipette was filled with the buffer solution. The reasoning was that the electrolytes should have been able to interact with the surface of the upper, clean part as well. But after seeing how the pipette looked in Figure 27B, it is believed that there may be an influence and that sandpapering the electrode would have helped against the resistance issues encountered.

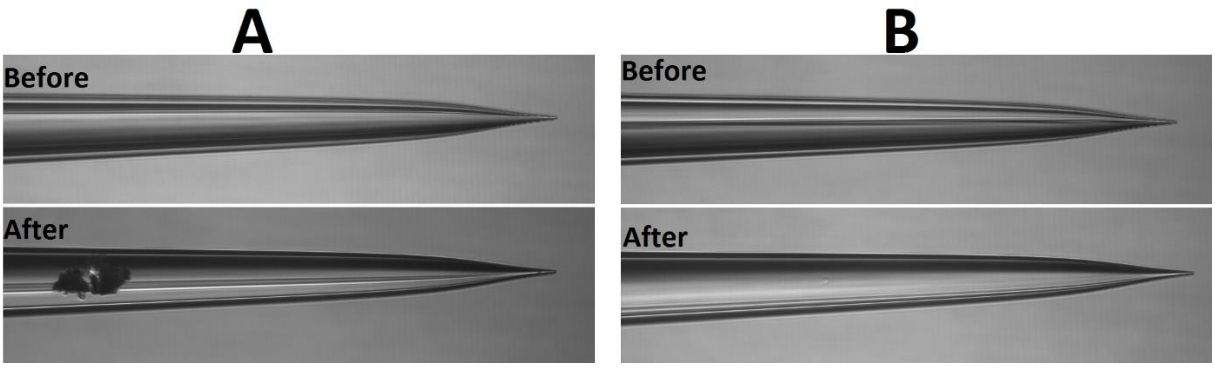

Figure 27: Two pipettes were tried for the trapping experiment. (A) Here we see the first pipette used and in the after-image that there is some particle clogging the pipette. (B) This is the second pipette without any visible blockage. The pipette was also checked downstream from the tip but no particle could be found.

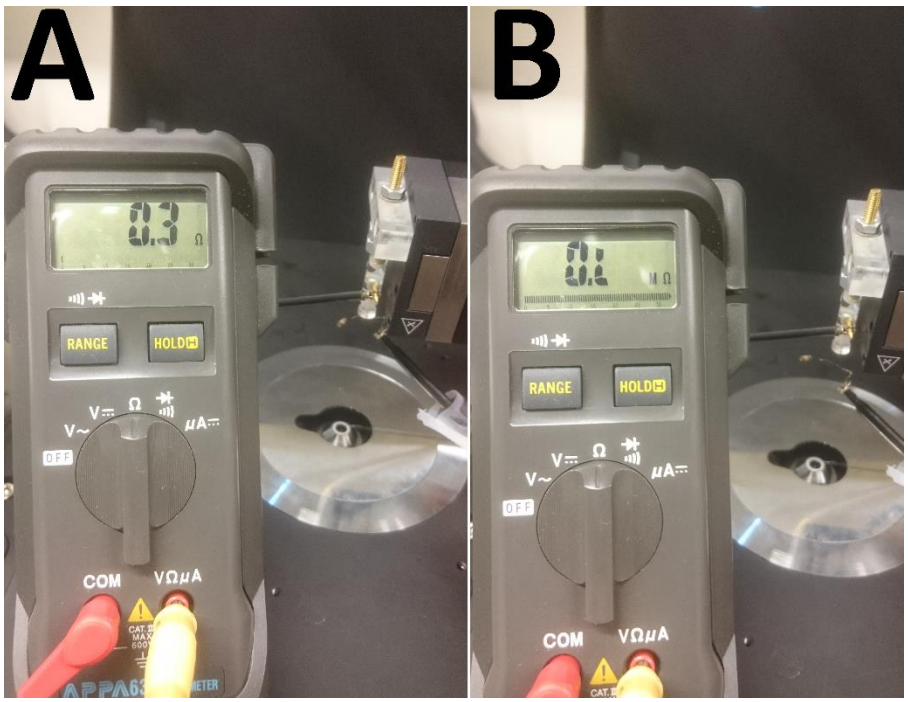

Figure 28: The resistance is measured going from the wire of the resistor carrying electrode to the piezo electrode wire. (A) Here, the wire touches the upper part of the piezo electrode, free from chloride bleaching, giving a low resistance of 0.3 Ohm. (B) Here, the wire touches the lower part which is exposed to bleaching which gives the O.L reading.

5 Conclusions and Future Work

From the data obtained, the height of the protruding CD45 molecules seemed to be affected by the salt concentration. However, the standard deviations of the 500 mM samples were quite high. Some of the problems that were encountered when determining the protein height could be alluded to having too long waiting times during some experiments and pipette issues. Blockages of the micropipette influenced the A_{hydro} curves need to fit the curves when doing further analysis. Also, replicating similar pipette sizes proved to be difficult using a flaming/brown micropipette puller. A better alternative would have been to use a laser based one which would have given more homogenous dimensions, and hopefully better tip openings. More runs would have need to be done in order to get a more reliable data set and the issues with the resistance and pipette blockages addressed.

Acknowledgements

I would like to thank my supervisor Dr. Peter Jönsson for providing me with the opportunity to do this thesis and for the encouragement and help during the last weeks of writing the thesis. I would also like to thank Victoria “Vicky” Junghans for taking her time to walk me through this challenging experiment and all of the programs used for analysing the data. The many tips I received helped a lot! I have learned a lot during these short 10 weeks. And thank you to the Department of Physical Chemistry for having me and to the people who provided me with some tips and tricks as well.

References

[1] V. T. Chang *et al.*, “Initiation of T cell signaling by CD45 segregation at ‘close contacts,’” *Nat. Immunol.*, vol. 17, no. 5, pp. 574–582, Mar. 2016.

[2] S. J. Davis and P. A. van der Merwe, “The kinetic-segregation model: TCR triggering and beyond.,” *Nat. Immunol.*, vol. 7, no. 8, pp. 803–809, 2006.

[3] J. R. James and R. D. Vale, “Biophysical mechanism of T-cell receptor triggering in a reconstituted system.,” *Nature*, vol. 487, no. 7405, pp. 64–69, Jul. 2012.

[4] E. T. Castellana and P. S. Cremer, “Solid supported lipid bilayers: From biophysical studies to sensor design,” *Surf. Sci. Rep.*, vol. 61, no. 10, pp. 429–444, Nov. 2006.

[5] L. Hirst, *Fundamentals of Soft Matter Science*, 1st ed. Boca Raton: CRC Press, 2013.

[6] D. Axelrod, “Total Internal Reflection Fluorescence Microscopy in Cell Biology,” *Traffic*, vol. 2, no. 11, pp. 764–774, Nov. 2001.

[7] S. J. Singer and G. L. Nicolson, “The fluid mosaic model of the structure of cell membranes.,” *Science*, vol. 175, no. 4023, pp. 720–31, Feb. 1972.

[8] A. Carisey, M. Stroud, R. Tsang, and C. Ballestrem, “Fluorescence recovery after photobleaching.,” *Methods Mol. Biol.*, vol. 769, pp. 387–402, 2011.

[9] X. Zhang, L. Ma, and Y. Zhang, “High-resolution optical tweezers for single-molecule manipulation.,” *Yale J. Biol. Med.*, vol. 86, no. 3, pp. 367–83, 2013.

[10] A. E. Cohen and W. E. Moerner, “Suppressing Brownian motion of individual biomolecules in solution,” *Proc. Natl. Acad. Sci.*, vol. 103, no. 12, pp. 4362–4365, 2006.

[11] H. M. Hertz, “Standing-wave acoustic trap for noninstrusive positiong of microparticles,” *J. Appl. Phys.*, vol. 78, no. 8, pp. 4845–49, 1995.

[12] P. Jönsson, J. McColl, R. W. Clarke, V. P. Ostanin, B. Jönsson, and D. Klenerman, “Hydrodynamic trapping of molecules in lipid bilayers.,” *Proc. Natl. Acad. Sci. U. S. A.*, vol. 109, no. 26, pp. 10328–33, Jun. 2012.

[13] P. Jönsson and B. Jönsson, “Hydrodynamic Forces on Macromolecules Protruding from Lipid Bilayers Due to External Liquid Flows,” *Langmuir*, vol. 31, no. 46, pp. 12708–12718, Nov. 2015.

[14] A. D. Edelstein, M. A. Tsuchida, N. Amodaj, H. Pinkard, R. D. Vale, and N. Stuurman, “Advanced methods of microscope control using μManager software,” *J. Biol. Methods*, vol. 1, no. 2, p. 10, 2014.

[15] P. Jönsson, M. P. Jonsson, J. O. Tegenfeldt, and F. Höök, “A Method Improving the Accuracy of Fluorescence Recovery after Photobleaching Analysis,” *Biophys. J.*, vol. 95, no. 11, pp. 5334–5348, Dec. 2008.